Available online at www.sciencedirect.com

ScienceDirect

journal homepage: www.elsevier.com/locate/burns

Warburg effect in keloids: A unique feature different from other types of scars

Zhiguo Su, Hu Jiao, Jincai Fan, Liqiang Liu, Jia Tian, Cheng Gan, Zengjie Yang, Tiran Zhang, Yihua Chen*

Ninth Department of Plastic Surgery, Plastic Surgery Hospital, Chinese Academy of Medical Sciences and Peking Union Medical College, Beijing, China

ARTICLE INFO

Article history:
Accepted 5 March 2021

Keywords:
Keloid
Glycometabolism
Warburg effect
Glycolysis

ABSTRACT

Keloid fibroblasts (KFs) undergo reprogramming of the metabolic phenotype from oxidative phosphorylation to the Warburg effect. However, more studies are needed to demonstrate whether there is a Warburg effect in KFs and to determine whether there is a similar phenomenon in other types of scars or in the proliferative stage of scars. In our study, the mRNA and protein expression of key glycolytic enzymes, glucose consumption and lactate production in KFs, normal skin fibroblasts (NFs), atrophic scar fibroblasts (ASFs), proliferative stage scar fibroblasts (PSSFs), and hypertrophic scar fibroblasts (HSFs) were detected. In addition, the effects of 2-deoxy-D-glucose (2-DG, a glycolysis inhibitor) on cell proliferation in KFs and NFs were studied. We found that the mRNA and protein expression of key glycolytic enzymes in KFs were significantly upregulated compared with those in NFs. Glucose consumption and lactate production in KFs were also higher than that in NFs. However, we found no similar phenomenon in ASFs, PSSFs, or HSFs. When treated with 2 mmol/l 2-DG, the cell viability of KFs decreased more than that of NFs. What's more, treatment with increasing concentrations of 2-DG could inhibit cell viability and migration of KFs in a dose-dependent manner. In conclusion, the Warburg effect in KFs is a feature different from ASFs, PSSFs, or HSFs. Keloids are essentially different from other types of scars in terms of energy metabolism. This characteristic of KFs could provide new hope for the early diagnosis and treatment of keloids.

1. Introduction

Keloids are part of a fibroproliferative disorder that occur in wounds as an exaggerated response to injury [1]. It can grow beyond the boundaries of the wound and will not regress spontaneously [2]. The lesions can cause pain, itching, and contracture, which becomes a cosmetic and psychological burden for patients [3]. However, there is no satisfactory treatment, as the key factor responsible for the disease process has not yet been identified [4,5].

In 1991, Sit [6] found that G6PDH activity in keloid fibroblasts (KFs) was significantly higher than that in normal skin fibroblasts (NFs) under oxygen saturation conditions. In 2006, Ozawa [7] performed positron emission tomography (PET) with fluorine-18-fluorodeoxyglucose (FDG) to examine glucose metabolism in keloids. Low-grade accumulation of FDG was observed in all lesions, indicating that glucose metabolism was accelerated in keloids. Vincent [8] reported in 2008 that KFs showed bioenergetics similar to cancer cells in generating ATP mainly from glycolysis. Recently, a study

* *Corresponding author.*
E-mail address: jiaohu2006@126.com (H. Jiao).
https://doi.org/10.1016/j.burns.2021.03.003
0305-4179/

performed by Li [9] also showed that the level of aerobic glycolysis was likely augmented in KFs compared to NFs. These studies demonstrated that KFs may undergo reprogramming of their metabolic phenotype from oxidative phosphorylation to the Warburg effect, similar to the Warburg effect in cancer cells.

However, more studies are needed to demonstrate if KFs undergo this metabolic reprogramming. In addition, it remains unknown whether there is a similar phenomenon in other types of scars or in the proliferative stage of scars. The aim of this study is to demonstrate whether there is a Warburg effect in KFs and to determine whether the Warburg effect is a metabolic pathway of keloids different from other types of scars.

2. Materials and methods

2.1. Patients and samples

Samples of normal human skin, atrophic scars, hypertrophic scars, proliferative stage scars, and keloids were obtained from patients of Plastic Surgery Hospital, Chinese Academy of Medical Sciences, and Peking Union Medical College. This research was approved by the Medical Ethics Committee (2018-8), and informed consent was obtained from all subjects.

Between March 2019 and August 2020, 15 keloid samples, 9 normal skin samples, 9 proliferative stage scar samples, 9 atrophic scar samples, and 9 hypertrophic scar samples were obtained. All subjects were Chinese and ranged in age from 7 to 52 years. Only clinically typical samples were included in this study. None of the patients had undergone radiotherapy or hormonotherapy. Additionally, normal skin samples were obtained from patients during unrelated surgical operations. Proliferative stage scars were defined as erythematous and pruritic tissue with slight elevation within 6 months of wound healing. Atrophic scars were characterized by flattened tissue with nearly normal skin appearance after 1 year of wound healing. Hypertrophic scars were elevated and confined to the borders of the burn injury or trauma after 1 year of wound healing. The keloid is elevated, invades surrounding tissue, and can grow and spread for years. The onset time of the keloids ranged from 1 year to 10 years. The tissues were collected in sterile bottles immediately after surgical removal and kept in the refrigerator at 4°C until processing, usually within 8 h.

2.2. Isolation and culture of cells

Briefly, the normal skin specimens were sectioned into 2–3 cm pieces and placed in 3 mg/ml Dispase II (Invitrogen, USA) in DMEM overnight at 4°C. Then, the epidermis was removed. The dermis or scar tissues were minced into pieces smaller than 1 mm^3. The pieces were exposed to 2 mg/ml collagenase type I (Sigma-Aldrich, USA) and incubated at 37°C for 3–4 h. After, the cell suspension was centrifuged at 1000 rpm for 5 min. The supernatant was discarded, and the cells were cultured in Dulbecco's modified Eagle's medium (DMEM; HyClone, USA) supplemented with 10% fetal bovine serum (FBS; Gibco, USA), 100 U/ml penicillin and 100 mg/ml streptomycin (HyClone, USA) in a humidified incubator containing 5% CO_2 at 37°C. Cells were used at passages 1–3 for experiments.

2.3. RNA extraction and quantitative real-time PCR (qPCR)

Total RNA was extracted using TRIzol reagent (Invitrogen, USA) according to the manufacturer's protocol. Then, 1 μg of total RNA was reverse transcribed into cDNA using the iScript cDNA synthesis kit (Bio-Rad, Hercules, USA). Then, qPCR was performed using an ABI Prism 7300 System (Applied Biosystems, USA) with SYBR Green Supermix (Invitrogen, USA). The mRNA expression levels of key glycolytic enzymes were detected, including hexokinase 2 (HK2), fructose-2,6-biphosphatase 3 (PFKFB3), pyruvate kinase isoform M 2 (PKM2), and lactate dehydrogenase A (LDHA). PCR primers were designed based on sequences from the corresponding genes (Table 1). β-Actin was used to normalize the results, and the relative expression level was calculated by using the 2^{-DDCt} cycle threshold method.

Table 1 – The primers for quantitative real-time PCR.

Gene		Primer sequence
β-Actin	Forward primer	5′-CTCCATCCTGGCCTCGCTGT-3′
	Reverse primer	5′-GCTGTCACCTTCACCGTTCC-3′
HK2	Forward primer	5′-GAGCCACCACTCACCCTACT-3′
	Reverse primer	5′-CCAGGCATTCGGCAATGTG-3′
PFKFB3	Forward primer	5′-TTGGCGTCCCCACAAAAGT-3′
	Reverse primer	5′-AGTTGTAGGAGCTGTACTGCTT-3′
PKM2	Forward primer	5′-ATGTCGAAGCCCCATAGTGAA-3′
	Reverse primer	5′-TGGGTGGTGAATCAATGTCCA-3′
LDHA	Forward primer	5′-ATGGCAACTCTAAAGGATCAGC-3′
	Reverse primer	5′-CCAACCCCAACAACTGTAATCT-3′
Type I Collagen	Forward primer	5′-CTG CAA GAA CAG CAT TGC AT-3′
	Reverse primer	5′-GGC GTG ATG GCT TAT TTG TT-3′
Type III Collagen	Forward primer	5′-GAC CCT AAC CAA GGA TGC AA-3′
	Reverse primer	5′-GGA AAT TCA GGA TTG CCG TA-3′
TGF-β1	Forward primer	5′-CAA GCA GAG TAC ACA CAG CA-3′
	Reverse primer	5′-GAT GCT GGG GCC CCT CTC CAGC-3′
α-SMA	Forward primer	5′-AAA AGA CAG CTA CGT GGG TGA-3′
	Reverse primer	5′-GCC ATG TTC TAT CGG GTA CTTC-3′

2.4. Protein extraction and western blot

Total cellular proteins were extracted using RIPA lysis buffer containing phosphatase and protease inhibitors (Applygen Technologies, China). The concentration of total protein was detected with a BCA Protein Assay kit (Applygen Technologies, China). Equal amounts (20 μg) of protein were separated using 10% SDS-PAGE gels. The proteins were then transferred to polyvinylidene difluoride membranes (0.45 mm; Solarbio, China). The membranes were blocked with 5% nonfat milk for 1 h at room temperature and incubated with primary antibodies (anti-HK2, anti-PFKFB3, anti-PKM2, anti-LDHA, and anti-β-actin rabbit monoclonal antibodies) (1:1000; Abcam, USA) at 4°C for 12 h. After washing, the membranes were incubated with goat anti-rabbit secondary antibodies (1:5000; Abcam, USA). Finally, the bands were visualized by enhanced chemiluminescence (ECL) detection system (Thermo Fisher Scientific, USA). The optical densities of the bands were quantified using a Gel Image system ver.4.00 (Tanon, China).

2.5. Glucose uptake and lactate production detection

For glucose uptake and lactate production assays, 1×10^5 cells were seeded onto 6-well plates in triplicate and cultured at 37°C. The culture medium was replaced the next day and collected after incubation for 48 h. Then, the glucose and lactate concentrations in the culture supernatant were determined according to the manufacturer's instructions. Glucose content was tested using a glucose assay kit (Jiancheng Bioengineering Institute, China). According to the directions, 10 μl cell culture supernatant was mixed with 1000 μl Glucose Assay Reagent and incubated at 37°C for 10 min. The absorbance at 340 nm was read on a microplate reader (Thermo Fisher Scientific, USA). Lactate content was tested using a lactic acid assay kit (Jiancheng Bioengineering Institute, China). Briefly, 10 μl of cell culture supernatant was mixed with the corresponding reagents and incubated at 37°C for 10 min. The absorbance at 530 nm was read on a microplate reader.

2.6. The effects of 2-deoxy-D-glucose (2-DG) on cell proliferation

Cells were seeded onto 96-well plates in triplicate at a density of 5×10^3 cells per well and cultured at 37°C. The next day, the cells were treated with 2-DG (Sigma-Aldrich, USA) at different concentrations (0, 2, 4, 8, 16, and 24 mmol/l) for 48 h. Then, cell viability was detected with a Cell Counting Kit-8 (CCK-8; Dojindo, Japan). According to the directions, 10 μl of CCK-8 reagent was added to each well and incubated at 37°C for 1.5 h. The absorbance at 450 nm was read on a microplate reader.

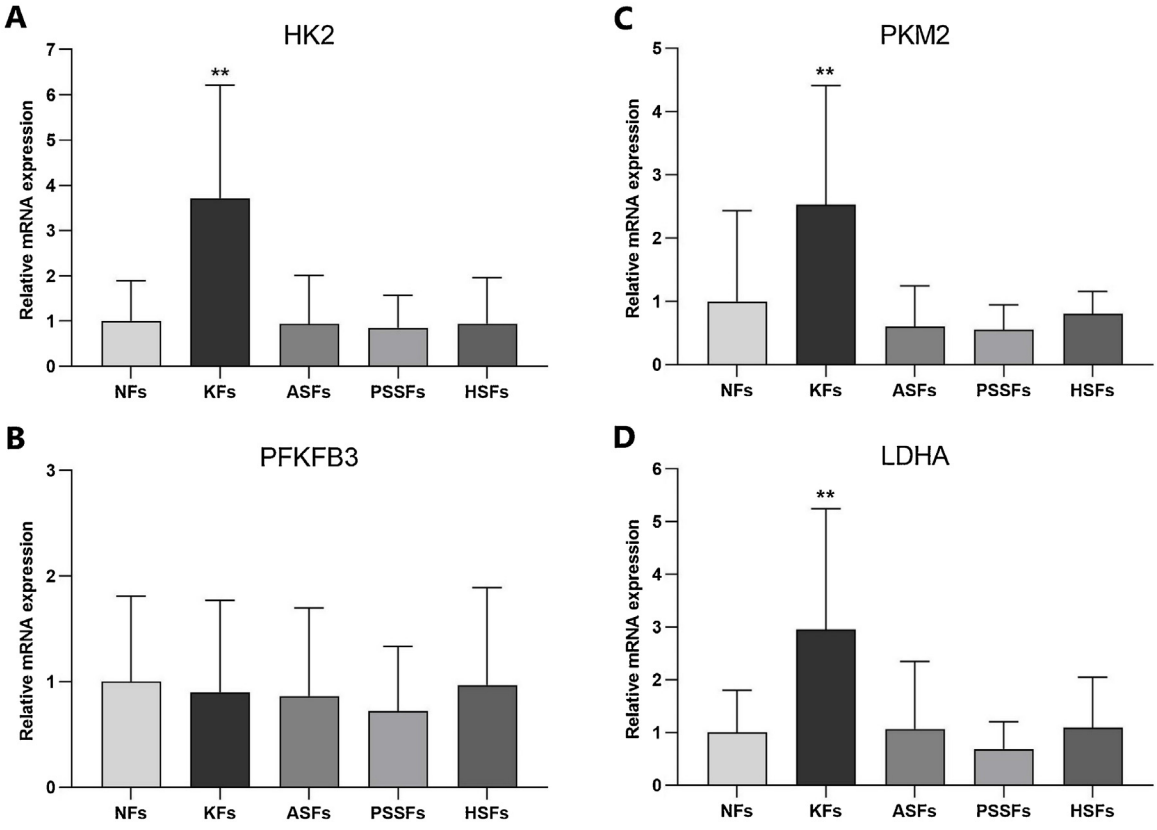

Fig. 1 – The mRNA expression of the HK2, PKM2 and ALDH genes in KFs was several times higher than that in the NF group (HK2: $^{**}p=0.002$; PKM2: $^{**}p=0.009$; LDHA: $^{**}p=0.006$). The mRNA expression of key glycolytic enzymes in atrophic scar fibroblasts (ASFs), proliferative stage scar fibroblasts (PSSFs) and hypertrophic scar fibroblasts (HSFs) were not significantly different from those in NFs ($p>0.05$).

2.7. Scratch wound assay

For scratch wound assay, KFs were seeded onto 6-well plates at a density of 2×10^5 cells per well and cultured at 37°C until they reached ~100% confluence. Then, a scratch wound was generated on the cell monolayer by a 200 μl tip. After washing with PBS in triplicate, the cells were incubated with DMEM (without FBS) containing 2-DG at different concentrations (0, 2, 4, 8, 16, and 24 mmol/l). Digital images of each wound were captured under a Nikon Eclipse E200 microscope (Nikon, Japan) immediately (0 h), 24 h, and 48 h after scratch generation. Pictures were captured from three random views. Cell migration was analyzed using the software Image J (National Institutes of Health, USA).

2.8. The effect of 2-DG on the collagen production of KFs

Briefly, KFs were seeded onto 6-well plates at a density of 1×10^5 cells per well and cultured at 37°C until they reached ~80% confluence. Following this, the cells were incubated with a complete medium containing 2-DG at different concentrations (0, 2, 4, 8, 16, and 24 mmol/l) for 24 h. Then, total RNA was extracted and RT-PCR was performed as above. The mRNA expression levels of type I collagen, type III collagen, TGF-β1, and α-SMA were detected. PCR primers were designed based on sequences from the corresponding genes (Table 1). β-Actin was used to normalize the results.

2.9. Statistical analysis

All experiments were performed in triplicate, and the data are expressed as the means ± standard deviation (SD). Statistical analyses were performed using SPSS 21.0 software. When the data fit the normal distribution, Student's *t*-test was used for comparison between two groups, and one-way ANOVA was selected for group comparisons. Otherwise, the Mann–Whitney *U* test or the Wilcoxon *W* test was used. $P<0.05$ was considered to be statistically significant.

3. Results

3.1. The mRNA expression and protein expression of key glycolytic enzymes

The transcription levels of key glycolytic enzyme genes in KFs were significantly upregulated compared with other groups except for PFKFB3 (Fig. 1). The mRNA expression of the HK2, PKM2 and ALDH genes in KFs was 3.72 ± 2.50, 2.53 ± 1.88, and 2.95 ± 2.29 times higher than that in the NF group, respectively ($p<0.01$ for all). The mRNA expression of key glycolytic enzymes in atrophic scar fibroblasts (ASFs), proliferative stage scar fibroblasts (PSSFs), and hypertrophic scar fibroblasts (HSFs) was not significantly different from those in NFs ($p>0.05$). The protein expression of the HK2, PKM2, and ALDH genes in the KFs group was also significantly upregulated compared with that in the NFs group ($p<0.01$ for all). The protein expression of key glycolytic enzymes in ASFs, PSSFs, and HSFs was not significantly different from that in NFs ($p>0.05$) (Fig. 2). This finding is consistent with the mRNA expression results.

3.2. Glucose consumption and lactate production

The uptake of glucose and the production of lactate in KFs, NFs, ASFs, PSSFs, and HSFs in 48 h were detected and compared (Fig. 3). Glucose consumption in KFs, NFs, ASFs, PSSFs, and HSFs were 7.12 ± 1.41 mmol, 5.09 ± 1.66 mmol, 5.29 ± 0.89 mmol, 4.12 ± 0.93 mmol, 4.23 ± 1.56 mmol, respectively. Glucose consumption in KFs was significantly higher than that in NFs ($p=0.004$). There was no significant difference in glucose consumption between ASFs and NFs, PSSF and NFs, or HSFs and NFs ($p>0.05$). Besides, lactate production in KFs, NFs, ASFs, PSSFs, and HSFs was 7.06 ± 2.32 mmol, 5.29 ± 0.91 mmol, 4.52 ± 0.98 mmol, 5.45 ± 0.87 mmol, 5.40 ± 1.55 mmol, respectively. Lactate production in KFs was significantly higher than that in NFs ($p=0.041$). Lactate production in ASFs, PSSF, and HSFs was not significantly different from that in NFs ($p>0.05$).

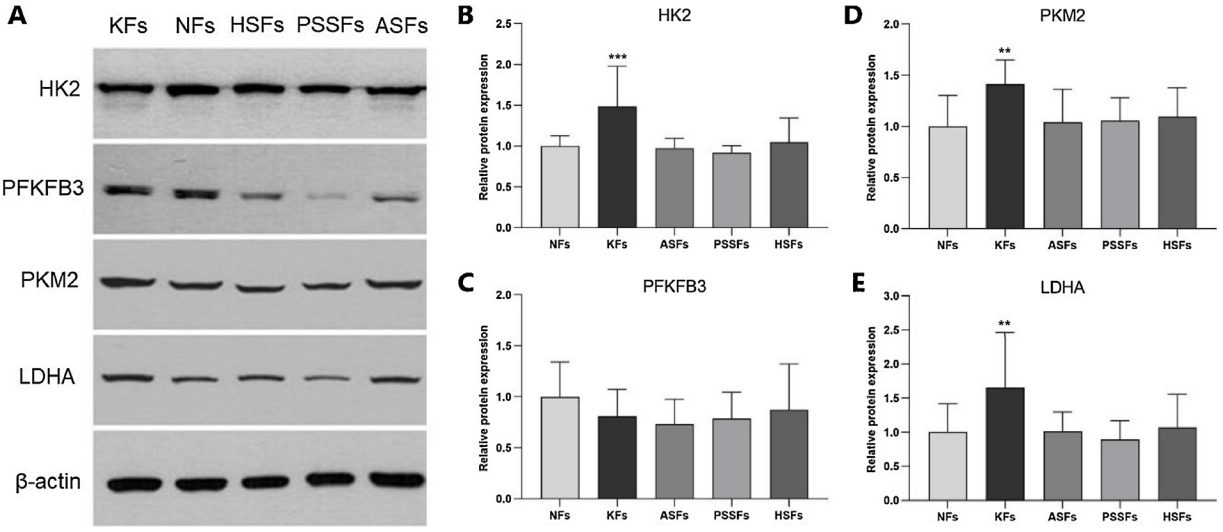

Fig. 2 – The protein expression of the HK2, PKM2, and ALDH genes in the KF group was significantly upregulated compared with that in the NF group (HK2: $^{***}p<0.001$; PKM2: $^{**}p=0.003$; LDHA: $^{**}p=0.009$). The protein expression of key glycolytic enzymes in ASFs, PSSFs and HSFs was not significantly different from that in NFs ($p>0.05$).

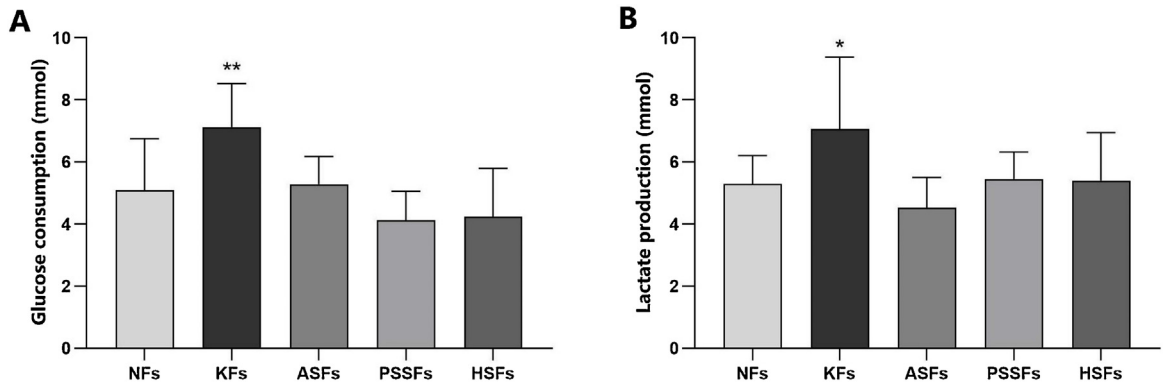

Fig. 3 – Glucose consumption and lactate production in each group. Glucose consumption and lactate production in KFs were both significantly higher than those in NFs ($p=0.004$, *$p=0.041$). There was no significant difference in glucose consumption or lactate production between ASFs and NFs, PSSF and NFs, or HSFs and NFs ($p>0.05$).**

3.3. *The effects of 2-DG on cell proliferation*

The effects of different concentrations of 2-DG (0, 2, 4, 8, 16, 24mmol/l) on cell proliferation in KFs and NFs were detected. The results showed that 2-DG could significantly inhibit cell viability in both KFs and NFs (Fig. 4). Treatment with increasing concentrations of 2-DG inhibited cell viability in both KFs and NFs in a dose-dependent manner. However, the decreasing trends of cell activity of KFs and NFs were not identical, especially when treated with 2mmol/l 2-DG. Compared with the control group (treated without 2-DG), when treated with 2mmol/l 2-DG, the cell viability of KFs decreased by 31.87 ±5.75%, while the cell viability of NFs decreased by 26.54 ±3.91%. The difference between the two was statistically significant ($p=0.025$). However, when treated with higher concentrations of 2-DG, the decreasing trends of cell activity of KFs and NFs became basically the same.

3.4. *The effects of 2-DG on the migration of KFs*

The scratch wound assay was used to evaluate the effects of 2-DG on the migration of KFs. As it turned out, 2-DG significantly inhibited KFs migration in a dose-dependent manner (Fig. 5). After 24h, KFs in the control group had migrated 48.89±17.94% of the scratched area, whereas 2mmol/l, 4mmol/l, 8mmol/l, 16mmol/l, and 24mmol/l – treated KFs had migrated 40.00 ±14.70%, 34.61±12.97%, 29.51±10.44%, 22.53±8.97%, and 13.71±7.77% respectively. There were significant differences between the 2-DG treated groups and the control groups ($p<0.001$ for all). Similarly, after 48h, KFs in the control group had migrated 87.68±24.37% of the scratched area, whereas 2mmol/l, 4mmol/l, 8mmol/l, 16mmol/l, and 24mmol/l – treated KFs had migrated 75.91±20.89%, 66.48±18.09%, 54.87±14.47%, 40.78±9.76%, and 22.26±8.95% respectively. The 2-DG treated groups had significant differences from the control groups ($p<0.001$ for all).

3.5. *The effects of 2-DG on the collagen production in KFs*

The effects of 2-DG on the expression of type I collagen, type III collagen, TGF-β1, and α-SMA was detected in KFs using qPCR. As shown in Fig. 6, the mRNA expression of type I collagen, type III collagen, TGF-β1, and α-SMA in 2mmol/l, 4mmol/l, 8mmol/l, 16mmol/l, and 24mmol/l – treated KFs all had no significant differences from that in KFs treated without 2-DG ($p>0.05$ for all).

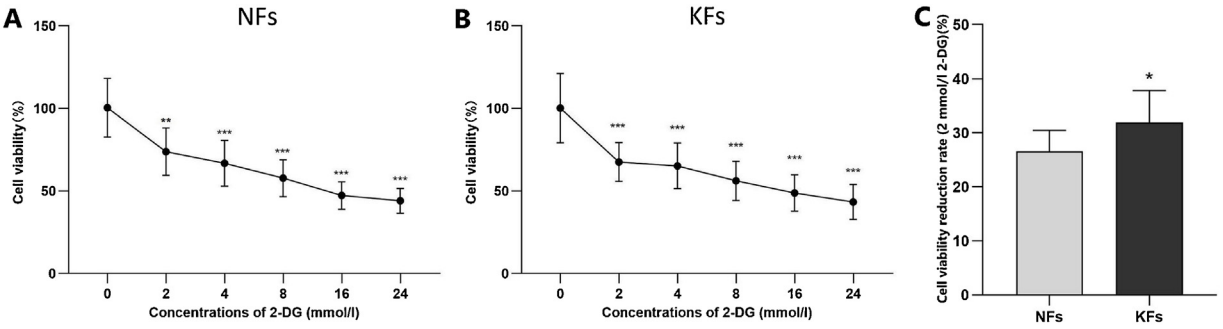

Fig. 4 – (A and B) The effect of different concentrations of 2-DG (0, 2, 4, 8, 16, 32mmol/l) on cell proliferation in KFs and NFs. Treatment with 2-DG significantly inhibited cell viability in both KFs and NFs, and treatment with increasing concentrations of 2-DG inhibited cell viability in both KFs and NFs in a dose-dependent manner ($p=0.008$, ***$p<0.001$). (C) The cell viability reduction rate of KFs and NFs when treated with 2mmol/l 2-DG. Compared with the control group (treated without 2-DG), when treated with 2mmol/l 2-DG, the cell viability of KFs decreased by 32.52%, while the cell viability of NFs decreased by 26.49%. The difference between the two was statistically significant ($p=0.025$).**

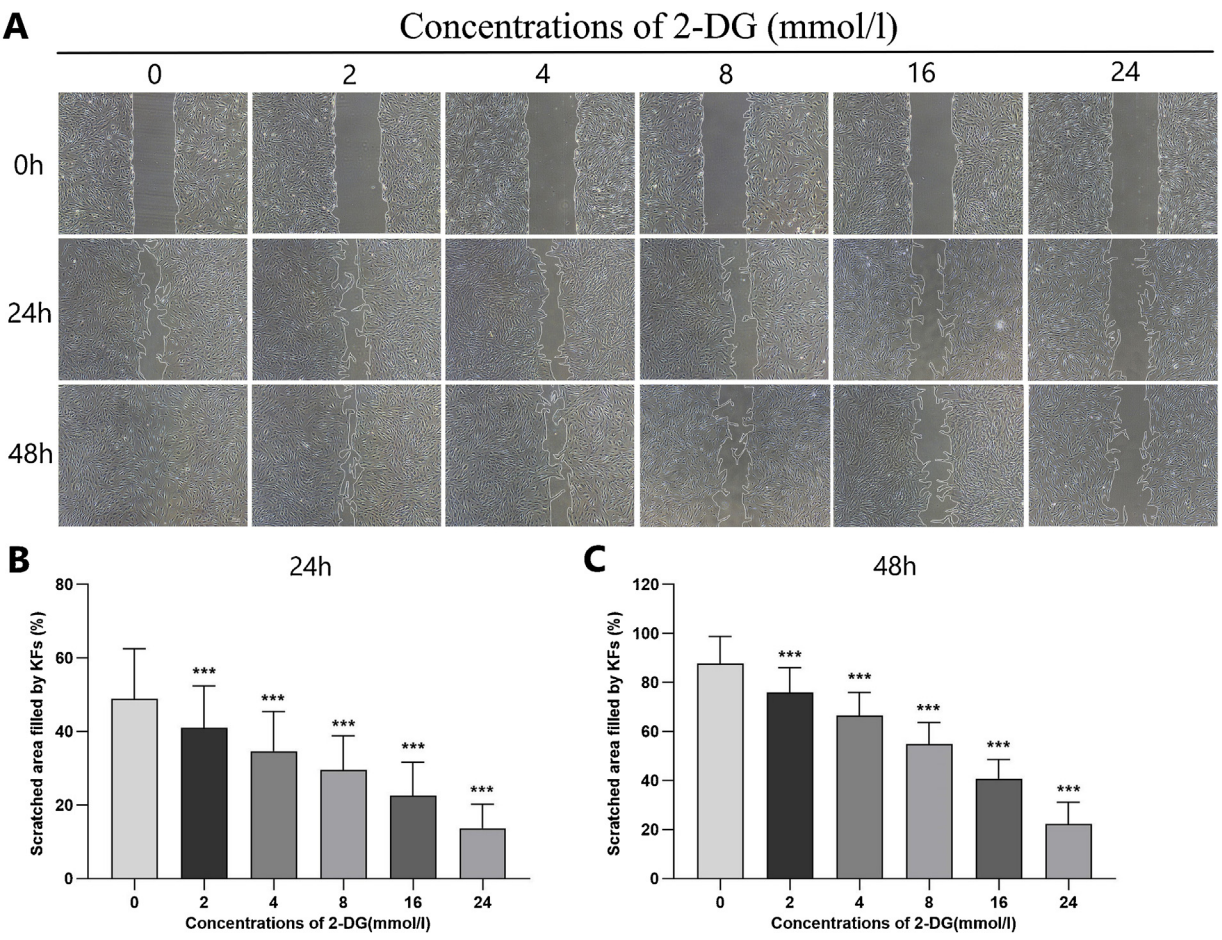

Fig. 5 – Results of scratch wound assay in KFs treated with different concentrations of 2-DG (0, 2, 4, 8, 16, and 24mmol/l). After 24h, KFs in the control group had migrated more of the scratched area than the 2-DG treated groups. The difference was statistically significant ($p < 0.001$ for all). After 48h, the 2-DG treated groups also had significant differences from the control groups ($p < 0.001$ for all). As it turned out, 2-DG significantly inhibited KFs migration in a dose-dependent manner.

It seems that 2-DG cannot inhibit or enhance the expression of type I collagen, type III collagen, TGF-β1, or α-SMA in KFs in vitro.

4. Discussion

Most normal cells rely primarily on oxidative phosphorylation for ATP generation. However, tumor cells show unique metabolic pathways and produce ATP mainly depending on glycolysis, even when the oxygen supply is sufficient. This phenomenon was first reported by Otto Warburg in 1956, the so-called "Warburg effect" [10]. The Warburg effect (aerobic glycolysis) allows tumor cells to gain a survival advantage [11]. It can provide cancer cells with enough energy and biosynthetic precursors [12]. In addition, turning off oxidative phosphorylation can avoid the production of oxygen-free radicals and escape apoptosis [13]. Keloids can continue to grow and invade the surrounding normal skin, which is similar to tumor cells. Some studies have shown that KFs may undergo reprogramming of their metabolic phenotype from oxidative phosphorylation to aerobic glycolysis [8,9]. However, the evidence is insufficient and more studies are needed to demonstrate this view. Besides, it is found that fibroblasts derived from lesions of fibrotic diseases, such as renal fibrosis, idiopathic pulmonary fibrosis, or laryngotracheal stenosis also embraced a similar energy metabolism shift toward glycolysis [14–16]. Therefore, this phenomenon may also exist in other types of scars or in the proliferative stage of scars.

In this study, the mRNA and protein expression of key glycolytic enzymes, glucose consumption, and lactate production in KFs, NFs, ASFs, PSSFs, and HSFs were detected. The results showed that KFs consume more glucose and produce more lactate than NFs. Moreover, the mRNA expression of key glycolytic enzymes in KFs, including HK2, PKM2, and ALDH, was significantly upregulated. The protein expression was consistent with the mRNA expression results. These findings coincided with the studies conducted by Li [9]. So, the glycolysis in KFs was enhanced and that aerobic glycolysis (Warburg effect) likely occurred in KFs. In addition, glucose consumption and lactate production in ASFs, HSFs, or PSSFs were not significantly upregulated compared with that in NFs. The mRNA and protein expression of key glycolytic enzymes in ASFs, HSFs, or PSSFs were also not significantly different from that in NFs. Therefore, ASFs, HSFs, or PSSFs do not undergo reprogramming of metabolic phenotypes as observed in KFs. Taken together, the Warburg effect in KFs is a special feature,

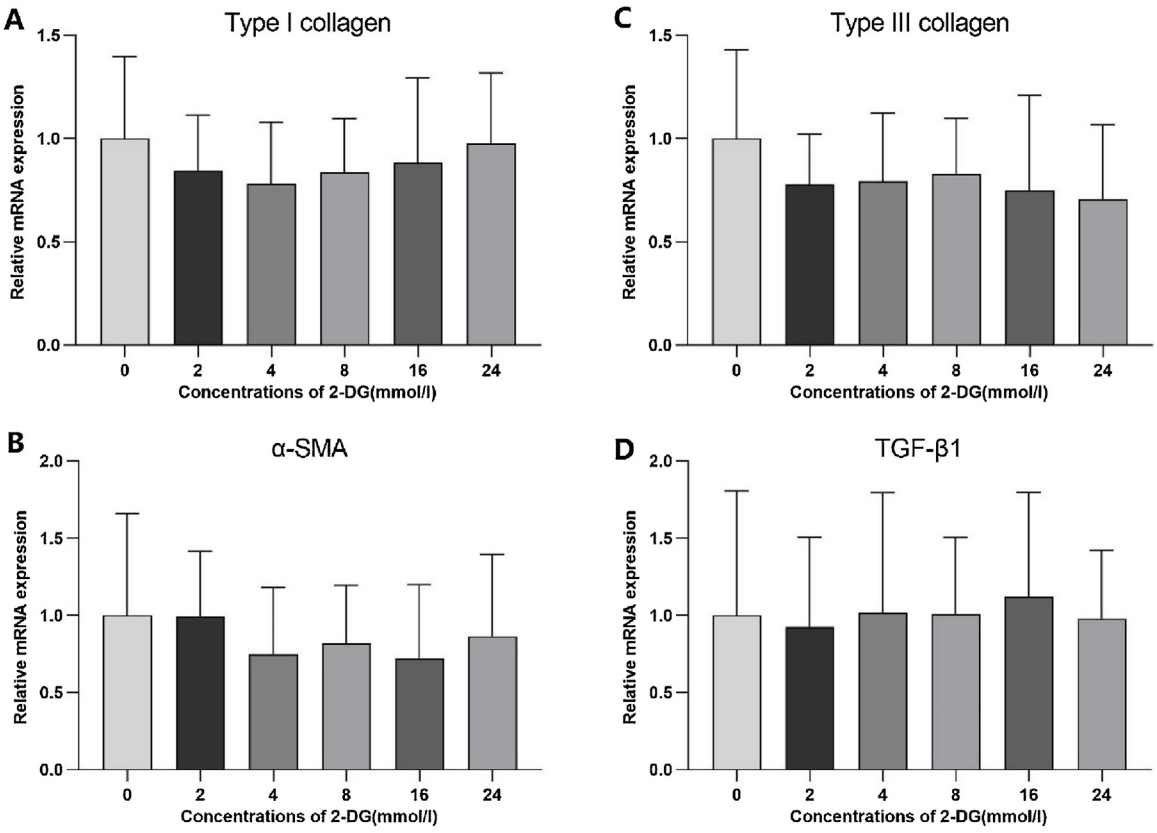

Fig. 6 – The effects of 2-DG on the collagen production in KFs. The results showed that the mRNA expression of type I collagen, type III collagen, TGF-β1, and α-SMA in 2mmol/l, 4mmol/l, 8mmol/l, 16mmol/l, and 24mmol/l – treated KFs all had no significant differences from that in KFs treated without 2-DG ($p > 0.05$ for all).

which does not exist in other types of scars or in the proliferative stage of scars. Keloids are essentially different from other types of scars in terms of energy metabolism.

Clinical diagnosis of keloids usually depends on the characteristics that can grow beyond the boundaries of the wound and it is difficult for early diagnosis. The Warburg effect in KFs could provide hope for the early diagnosis of keloids. The enhanced glycolysis may be detected by certain means to distinguish keloids for early diagnosis in the future. For example, Ozawa [7] found that glucose consumption was accelerated in keloids by using positron emission tomography (PET). Therefore, it helps to detect the glucose consumption or other elements related to glycolysis in lesions to distinguish keloids with PET or a more precise instrument in the future.

Through complete oxidative phosphorylation, the metabolism of one molecule of glucose can produce 36 ATPs. In contrast, the glycolysis pathway can only produce 2 ATPs, which is less efficient [11]. If KFs rely entirely on glycolysis for their energy supply, KFs would consume several times more glucose and produce several times more lactate than NFs, similar to tumor cells [17]. However, the glucose uptake and lactate production of KFs in our study were less than twice that of NFs, which was similar in the studies of Li [9]. Therefore, both aerobic glycolysis and oxidative phosphorylation occur in KFs. This finding is consistent with the fact that only low-grade accumulation of fluorine-18-fluorodeoxyglucose (FDG) was observed in keloids, which is different from tumors [7,11].

In our study, the effects of a glycolysis inhibitor (2-DG) on cell proliferation in KFs and NFs were detected. The results showed that 2-DG could significantly inhibit cell viability in both KFs and NFs in a dose-dependent manner. When treated with 2mmol/l 2-DG, the cell viability of KFs decreased more pronounced than NFs. So, compared with NFs, KFs is more dependent on glycolysis. This is another evidence for enhanced glycolysis in KFs. However, when treated with higher concentrations of 2-DG, the decreasing trends of cell activity of KFs and NFs became basically the same. In general, the differences between the effects of 2-DG on cell viability of KFs and NFs is not that big. We speculate that this is because when treated with 2-DG, not only glycolysis but also oxidative phosphorylation in both KFs and NFs were affected, as glycolysis is the basis of oxidative phosphorylation and provides raw materials (pyruvate) for it.

To further investigate the relationship between the Warburg effect and the biological behavior of KFs, the cell migration and the collagen production in KFs were detected after the Warburg effect was inhibited by 2-DG. The results showed that 2-DG could significantly inhibit KFs migration in a dose-dependent manner. However, it seems that 2-DG had no significant influence on the expression of type I collagen, type III collagen, TGF-β1, or α-SMA in KFs in vitro. Given the collagen production decreased when KFs lost their original microenvironment in vitro, whether 2-DG could affect the collagen production of KFs in vivo needed further study [18]. Ding [15] demonstrated that inhibiting the Warburg effect

could suppress renal interstitial fibroblast activation and renal fibrosis. Similarly, we found that the glycolysis inhibitor could inhibit both cell viability and migration of KFs in a dose-dependent manner. Therefore, targeting glycolysis holds great promise in keloid treatment, and further mechanistic studies are currently underway.

However, the study has its own limitations. Firstly, the range of the onset time of the keloids is long (1 year to 10 years). Secondly, there is no normal skin sample obtained from the same patient with keloid. Thirdly, the magnitude of differences between strains is relatively small. Therefore, more researches are needed to study the metabolic reprogramming of KFs.

In conclusion, there is both aerobic glycolysis and oxidative phosphorylation in KFs, and there is no similar phenomenon in HSFs, ASFs, or PSSFs. The Warburg effect in KFs is a special feature, which does not exist in other types of scars or in the proliferative stage of scars. Therefore, keloids are essentially different from other types of scars in terms of energy metabolism. This characteristic in KFs could provide new hope for the early diagnosis and treatment of keloids.

Conflicts of interest

None declared.

Acknowledgment

This study was supported by the National Natural Science Foundation of China (No. 1110318021).

REFERENCES

[1] Unahabhokha T, Sucontphunt A, Nimmannit U, Chanvorachote P, Yongsanguanchai N, Pongrakhananon V. Molecular signalings in keloid disease and current therapeutic approaches from natural based compounds. Pharm Biol 2015;53:457–63.
[2] Wu X, Bian D, Dou Y, Gong Z, Tan Q, Xia Y, et al. Asiaticoside hinders the invasive growth of keloid fibroblasts through inhibition of the GDF-9/MAPK/Smad pathway. J Biochem Mol Toxic 2017;31:e21922.
[3] Lyons AB, Peacock A, Braunberger TL, Viola KV, Ozog DM. Disease severity and quality of life outcome measurements in patients with keloids. Dermatol Surg 2019;45:1477–83.
[4] He Y, Deng Z, Alghamdi M, Lu L, Fear MW, He L. From genetics to epigenetics: new insights into keloid scarring. Cell Proliferat 2017;50:e12326.
[5] Zhang Y, Zhang L, Lin X, Li Z, Zhang Q. Knockdown of IRF3 inhibits extracellular matrix expression in keloid fibroblasts. Biomed Pharmacother 2017;88:1064–8.
[6] Sit KH, Lau YK, Aw SE. Differential oxygen sensitivities in G6PDH activities of cultured keloid and normal skin dermis single cells. J Dermatol 1991;18:572–9.
[7] Ozawa T, Okamura T, Harada T, Muraoka M, Ozawa N, Koyama K, et al. Accumulation of glucose in keloids with FDG-PET. Ann Nucl Med 2006;20:41–4.
[8] Vincent AS, Phan TT, Mukhopadhyay A, Lim HY, Halliwell B, Wong KP. Human skin keloid fibroblasts display bioenergetics of cancer cells. J Invest Dermatol 2008;128:702–9.
[9] Li Q, Qin Z, Nie F, Bi H, Zhao R, Pan B, et al. Metabolic reprogramming in keloid fibroblasts: aerobic glycolysis and a novel therapeutic strategy. Biochem Biophys Res Commun 2018;496:641–7.
[10] Warburg O. On the origin of cancer cells. Science 1956;123:309–14.
[11] Kobayashi Y, Banno K, Kunitomi H, Takahashi T, Takeda T, Nakamura K, et al. Warburg effect in gynecologic cancers. J Obstet Gynaecol Res 2019;45:542–8.
[12] Zhai X, Yang Y, Wan J, Zhu R, Wu Y. Inhibition of LDH-A by oxamate induces G2/M arrest, apoptosis and increases radiosensitivity in nasopharyngeal carcinoma cells. Oncol Rep 2013;30:2983–91.
[13] Yu W, Yang Z, Huang R, Min Z, Ye M. SIRT6 promotes the Warburg effect of papillary thyroid cancer cell BCPAP through reactive oxygen species. Onco Targets Ther 2019;12:2861–8.
[14] Xie N, Tan Z, Banerjee S, Cui H, Ge J, Liu R, et al. Glycolytic reprogramming in myofibroblast differentiation and lung fibrosis. Am J Respir Crit Care 2015;192:1462–74.
[15] Ding H, Jiang L, Xu J, Bai F, Zhou Y, Yuan Q, et al. Inhibiting aerobic glycolysis suppresses renal interstitial fibroblast activation and renal fibrosis. Am J Physiol-Renal 2017;313:F561–75.
[16] Ma G, Samad I, Motz K, Yin LX, Duvvuri MV, Ding D, et al. Metabolic variations in normal and fibrotic human laryngotracheal-derived fibroblasts: a Warburg-like effect. The Laryngoscope 2017;127:E107–13.
[17] Bi Y, Han W, Li R, Wang Y, Du Z, Wang X, et al. Signal transducer and activator of transcription 3 promotes the Warburg effect possibly by inducing pyruvate kinase M2 phosphorylation in liver precancerous lesions. World J Gastroenterol 2019;25:1936–49.
[18] Jiao H, Dong P, Yan L, Yang Z, Lv X, Li Q, et al. TGF-β1 induces polypyrimidine tract-binding protein to alter fibroblasts proliferation and fibronectin deposition in keloid. Sci Rep-UK 2016;6:38033.